Band structure of face-centered and body-centered-cubic 3d transition metals

A. J. McAlister, J. R. Cuthill, R. C. Dobbyn,† and M. L. Williams
Institute for Materials Research, National Bureau of Standards, Gaithersburg, Maryland 20760

R. E. Watson‡
Brookhaven National Laboratory, Upton, New York 11973*
(Received 10 June 1974)

Measurements of the soft-x-ray $M_{2,3}$ emission spectra of face-centered Fe and Co, and body-centered Fe, Cr, and V are reported and M_3 single-hole excitation profiles are estimated. 3d bandwidths inferred from these results and earlier data on Cu and Ni are compared with band-theory predictions. As has been seen previously with x-ray and ultraviolet photoemission, the experimental Ni bandwidth is markedly narrower than theory predicts; there is a suggestion that the bandwidth of Cu is somewhat broader; theory and the present results are in fair agreement for the other metals. Fine structure is seen in the spectra; correlations are noted in the weak structure of metals of common crystal structure; and structural correlations with x-ray and ultraviolet photoemission data are seen as well.

I. INTRODUCTION

In recent years, notable progress has been made in understanding the electronic structure of transition and noble metals. For example, a number of Fermi surfaces have been successfully reproduced by energy-band calculations[1–6]; studies of several materials by deep-band-probe methods—soft-x-ray emission (SXS), ultraviolet (UPS) and x-ray (XPS) photoemission spectroscopies—are in some agreement with each other, [7–10] and in turn, with densities of states predicted by band theory. [8,11–13] Nonetheless, our over-all knowledge of such fundamental quantities as the width of the d bands, their placement with respect to, and degree of hybridization with the conduction band is imprecise, and in a few cases, entirely lacking. The present work is an attempt to improve and clarify the experimental situation by new measurements of the soft-x-ray $M_{2,3}$ emission spectra (valence band 4s, 3d to inner level 3p transition) of several cubic 3d metals: bcc Fe, [14] Cr, and V, fcc Fe and Co. The use of photon-counting techniques has enabled us to establish the existence of fine structure in the spectra. The single-hole M_3 profiles have been extracted from the $M_{2,3}$ spectral complexes in a plausible way. These results, together with earlier data on[8] Cu and[15] Ni, are intercompared for a given crystal structure, as a function of electron-per-atom ratio, and in turn, compared with the predictions of band theory. Structural correlations are observed among the experimental M_3 profiles for metals of common crystal structure and between these profiles and d-band state densities computed theoretically and inferred experimentally from UPS and XPS spectra. Trends in over-all d-band widths are in general agreement with theory save that the Ni width is too small, in fact smaller than that for Cu. The fact that Ni is anomalous has previously been seen in XPS[16] and UPS[17] spectra; whether it is associated with this metal's ferromagnetism remains to be seen.

With the exception of the bandwidth trend, the observations made in this paper are associated with weak structure seen in the spectra. Questions, such as whether the structure arises from experimental artifact, are therefore discussed in some detail. We should note that SXS differs from photoemission measurements in a variety of ways. It has a deep core hole in its initial state whereas photoemission starts in the ground state. Not being limited by a photoelectron escape depth, SXS probes deeper into the sample making it less susceptible to surface contamination (and thus less useful as a surface probe).

II. EXPERIMENTAL DETAILS

The samples studied were polycrystalline rods. Purity, sample temperature, exciting-electron-beam energy, and sample-chamber pressure range during measurements are listed in Table I. The spectrometer, a vacuum Rowland mount employing a glass grating, photoelectric detection, and digital data recording, has been described elsewhere. [15,18] Our practice is to mount a sample on an insulating block, with electrical contact made through a single thin wire. High temperatures (which, as we shall see in the Appendix, combine with low pressure and the action of the electron beam to provide a measure of surface cleanup) can then be achieved through the action of the exciting electron beam only. Where direct temperature measurements were made, a Pt–Pt-10%-Rh thermocouple was used. It was peened into a narrow hole bored into the rear of the specimen along a diameter and projecting to within ~$\frac{1}{16}$ in. of the front surface where the electron beam is striking. As we have argued earlier, [15] this arrangement should yield a reason-

TABLE I. Sample temperatures, stated purities, exciting-electron-beam voltages, and pressure range in sample chamber during measurements.

Sample	T (°C)	Stated purity (%)	Electron-beam energy (keV)	Pressure range (Torr)
Fe	560±5[a]	99.999[c]	2.5	1×10^{-7} to 4×10^{-8}
Fe	960±5[a]	99.999[c]	2.9	2×10^{-7} to 3×10^{-8}
Cr	560±5[a]	99.99[d]	2.4	1×10^{-7} to 8×10^{-8}
Co	780±20[b]	99.999	2.4	1×10^{-7} to 5×10^{-8}
V	900±20[b]	99.98	2.9	2×10^{-7} to 3×10^{-8}

[a] Measured with Pt–Pt-10%-Rh thermocouple.
[b] Estimated from thermal response of other materials having the same sample geometry, at the given excitation conditions.
[c] All Fe measurements made on one sample.
[d] Arc melted from 99.99% stock and cast as rod.

ably accurate estimate of the temperature in the active region of the sample. In two cases, Co and V, no thermocouple was attached. Temperatures were estimated from the known response of other samples at given excitation conditions. In all cases, the electron beam was incident at approximately 20° from the sample surface. X-ray takeoff was at 90°. The spectra were swept repetitively, the total photon count being recorded over successive short time intervals. Successive runs were summed to enhance the signal-to-noise ratio. Instrumental resolution, a function of both instrumental parameters and the length of the counting interval used, was approximately 0.2 eV for these measurements. Samples were machined lightly, then washed in acetone and freon before mounting in the sample chamber. Thus a thin oxide layer and coldwork damage were certainly present on the sample surfaces before the start of measurements. Also, carbon buildup at the surface was anticipated, owing to the deposition of cracked-pump oil vapor on the sample by the electron beam. The possibility that the present measurements are biased by these difficulties can be ruled out in the case of the Fe measurements, and shown to be minimal for the Cr measurements. (See Appendix for details.) The Co and V data are presented with reservations as to the cleanliness of the surface studied.

III. DATA ANALYSIS

The data obtained in the present investigation are displayed in Figs. 1–5. In each case, the upper curve is raw measured data, the bar length denoting 70% confidence level ($\pm N^{1/2}$, where N is the total number of counts accumulated at a given photon energy), while the lower curve shows smoothed[19] background-corrected data. The peak regions and lower energies, i.e., to the left of the peaks, are of primary interest. The smoothed curves display considerable weak structure and much of this lies within the noise. The structural features, in which we have greatest confidence, are marked by the brackets in the figures. Some of the structure is better established than the plotted spectra seem to indicate, because in some runs more channels of data were taken (and subsequently added together to improve statistics) than are plotted. For example, the notch in the bcc-Fe peak (Fig. 1) occurred in three adjacent channels in the original data though it appears in but one of the merged channels of the figure.

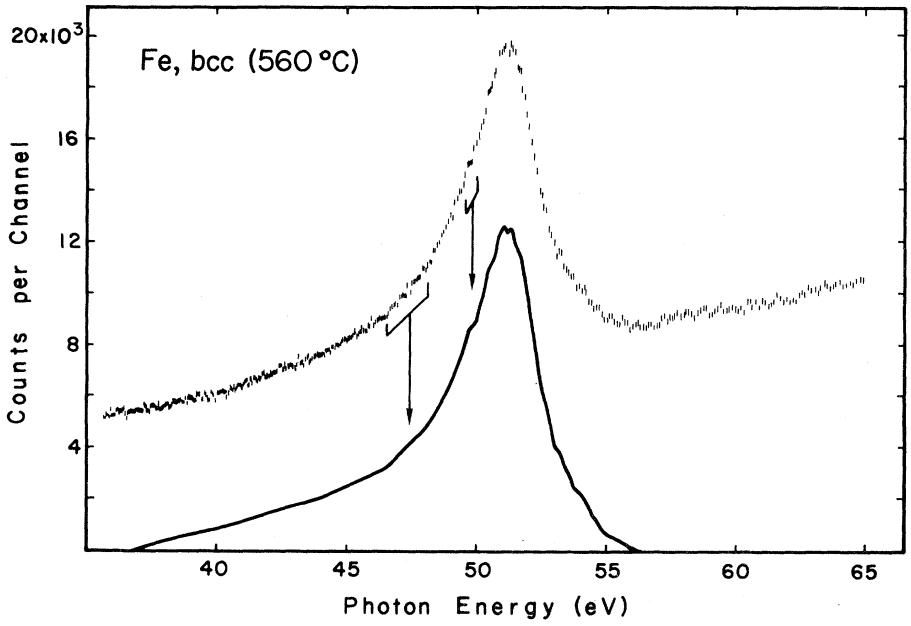

FIG. 1. Upper curve, raw $M_{2,3}$ spectrum of bcc, ferromagnetic Fe at 560 °C. Lower curve, smoothed background-corrected spectrum. Brackets indicate best characterized fine structure.

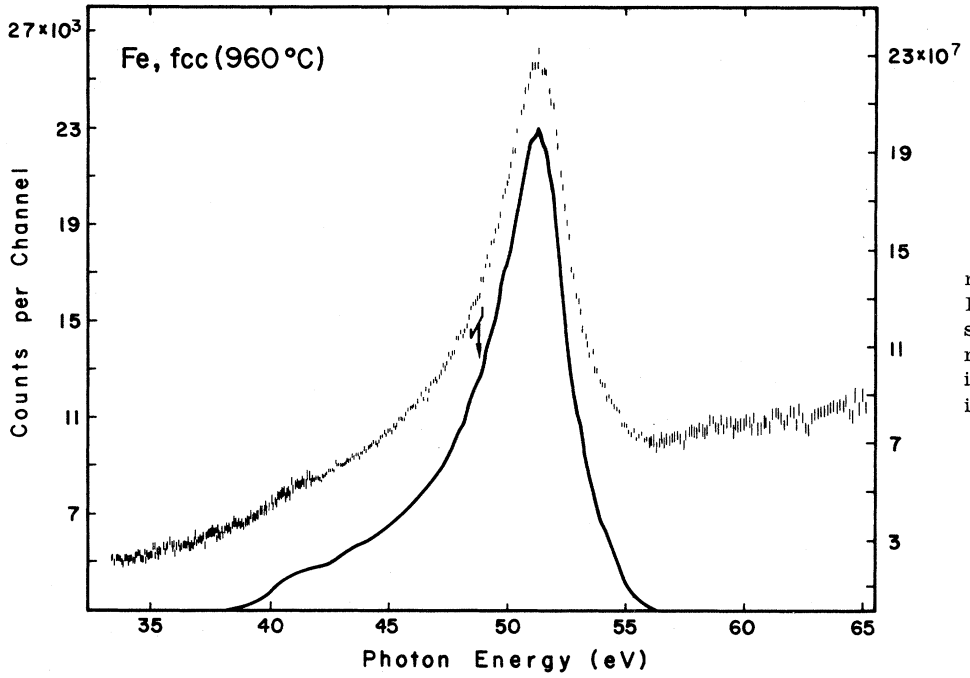

FIG. 2. Upper curve, raw $M_{2,3}$ spectrum of fcc Fe at 960 °C. Lower curve, smoothed background-corrected spectrum. Bracket indicates best characterized fine structure.

From the smoothed background-corrected curves, estimates were made of the single-hole M_3 emission profiles by a technique described in detail in our earlier study of the $M_{2,3}$ band of Cu, [8] where full details and a rationalization of the procedure are given. It assumes that the major components of a $3d$-metal $M_{2,3}$ spectral complex have the same shape and that the two principal components come from conduction-band filling of spin-orbit-split $3p_{3/2}$ and $3p_{1/2}$ holes. The reduction scheme works because of the dominance of the M_3 component associated with $3p_{3/2}$ filling. The two-to-one degen-

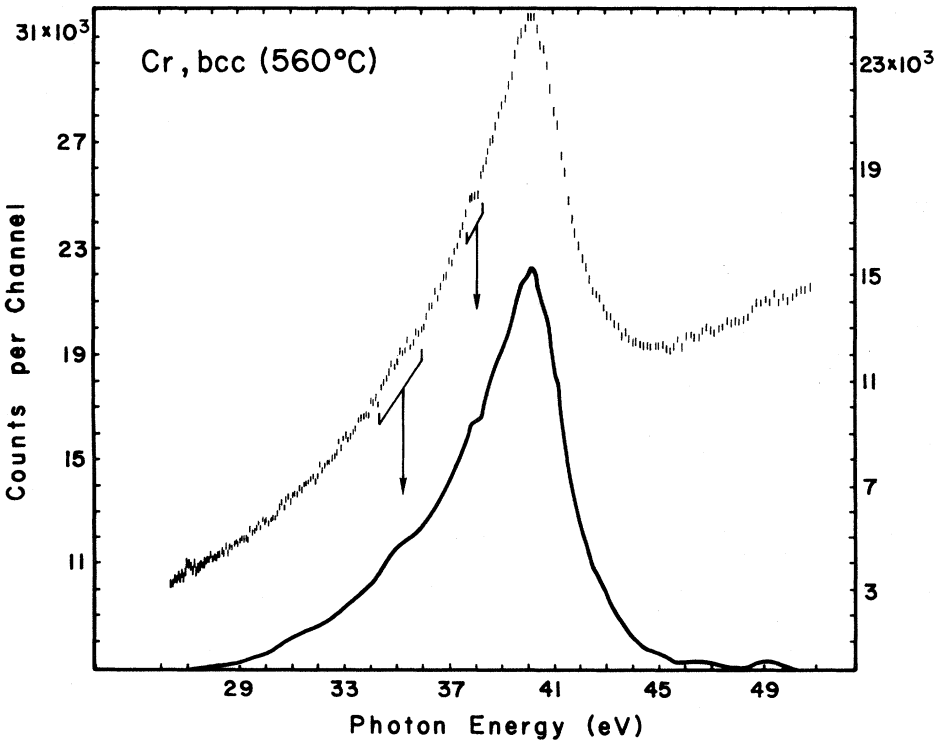

FIG. 3. Upper curve, raw $M_{2,3}$ spectrum of Cr at 560 °C. Lower curve, smoothed background-corrected spectrum. Brackets indicate best characterized fine structure.

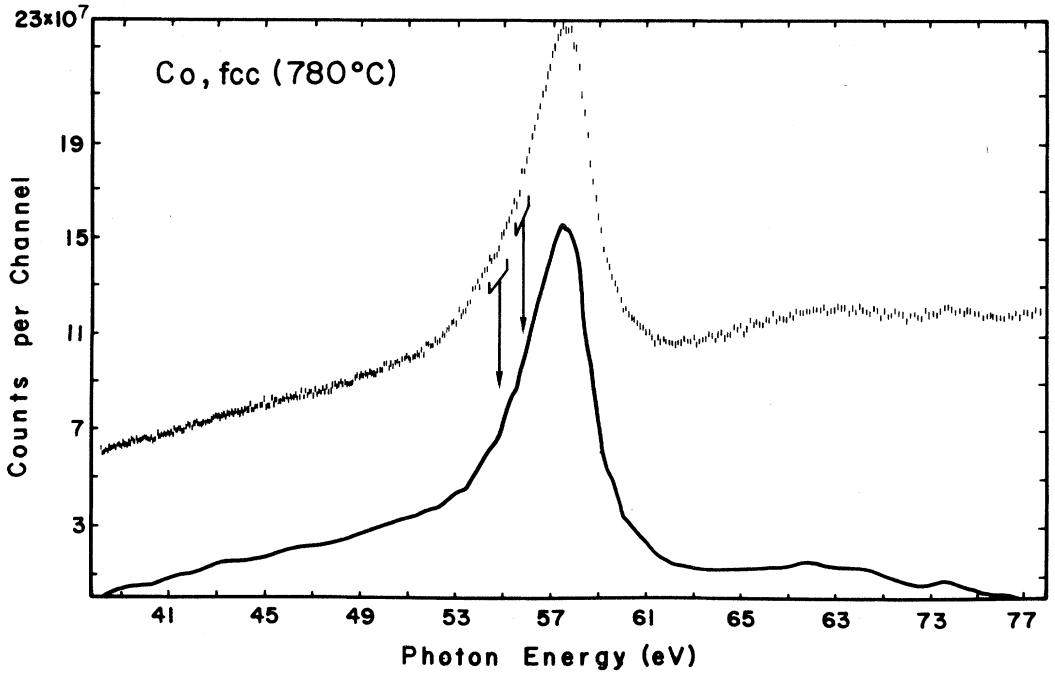

FIG. 4. Upper curve, raw $M_{2,3}$ spectrum of fcc Co at 780 °C. Lower curve, smoothed background-corrected spectrum. Brackets indicate best characterized fine structure. The slope break associated with the higher-energy bracket is the weakest of the structures flagged in Figs. 1–5.

eracy of $p_{3/2}$ vs $p_{1/2}$ suggests that the M_3 should have twice the intensity of the M_2, as it does in Cu. Auger processes where the $p_{3/2}$ fills a $p_{1/2}$ hole and a conduction electron is promoted to above the Fermi level E_F further reduce the relative M_2 intensity. This is particularly so in the transition metals, where there are ample numbers of available states above E_F. Because of the dominance of the M_3 component, the structural features to the left of the peaks of the smoothed curves in Figs. 1–5 are *neither created nor erased* on going to the M_3 profiles plotted in Figs. 6 and 7. The structure *appears sharper*, and its shape in the peak region *appears to change*, in the M_3 profiles because of the flattening attendant with subtracting out the downward-sloping M_2 curves.

The assumption that the $3p$ holes are simply spin-orbit split into two components is obviously a poor one for Fe, Co, and Ni, where there should be significant $3p$-$3d$ exchange splitting arising from the $3d$ moments. Attempting to account for this is at best difficult, for the $3p$ soft-x-ray photoelectron spectra obtained for these metals can be fitted as well with two lines as with more. This matter is not serious for the present inversion scheme because for these, like the metals without strong $3d$-$3p$ exchange, one component dominates the spectrum.

The broad low-energy tails of Figs. 6 and 7 are characteristic of SXS M_3 spectra, one possible source being energy-loss satellites. The loss data[20] of Robins and Swann are used to indicate where such satellites are expected to occur in the M_3 profiles of Figs. 6 and 7. The effects of other non-band-structure contributions to the M_3 spectra are thought to be minimal.[21]

IV. REPRODUCIBILITY OF SPECTRA

The Cu spectrum was rescanned and compared with that published previously.[8] Since the earlier

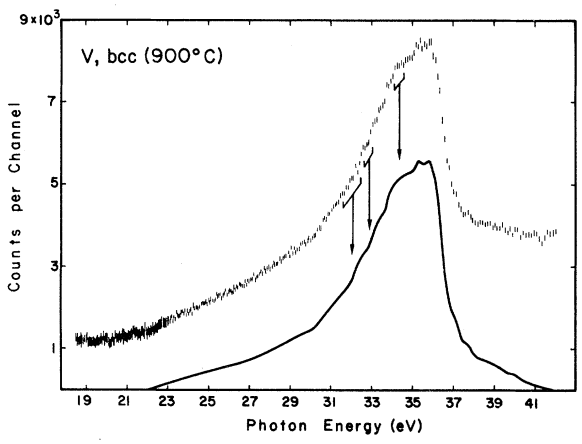

FIG. 5. Upper curve, raw $M_{2,3}$ spectrum of V at 900 °C. Lower curve, smoothed background-corrected spectrum. Brackets indicate best characterized fine structure.

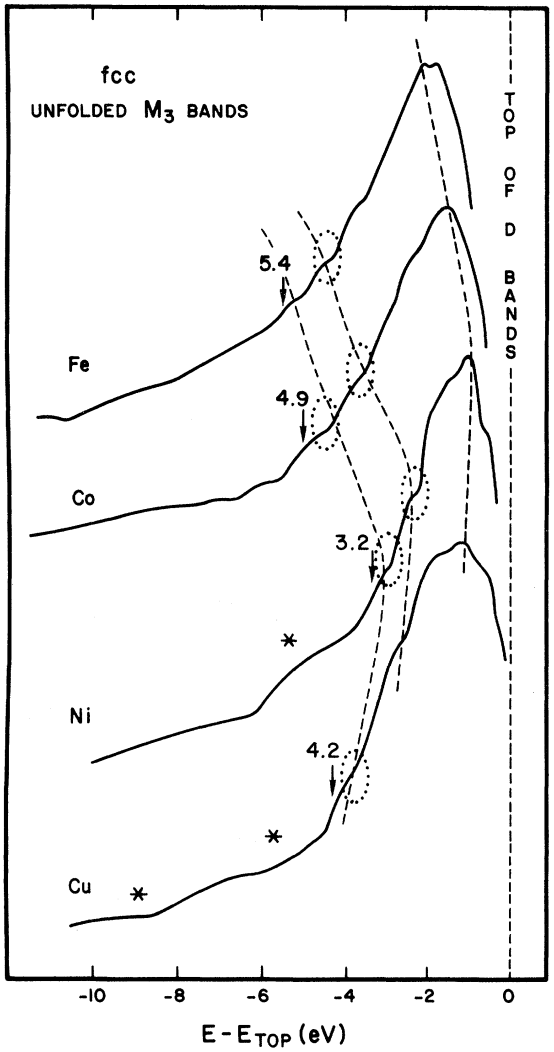

FIG. 6. Comparison of the unfolded M_3 bands of fcc Fe, Co, Ni (Ref. 15), and Cu (Ref. 8). The zero of energy is the d-band top as estimated in the text. Dashed lines connecting the profiles indicate the suggested structural correlation. The dotted ovals identify best characterized structure in the raw $M_{2,3}$ spectra. Arrows denote estimated d-band bottom and are labeled with total estimated d-band width. Stars denote expected position of energy-loss satellites.

study of Cu and measurements reported here, the instrument had been modified; in particular, the detector was changed. The new detector, while much more efficient, does not have a completely smooth response curve. The implications of this were accounted for by scanning the continuum of other metals having no characteristic structure in the photon energy region relevant to Cu. While the observed background structure slightly distorts the measured Cu spectrum, it does not correlate in energy with any structure in the Cu $M_{2,3}$ spectrum observed previously. (Our earlier detector had a smooth response in this region.) Allowing for the continuum distortion we find that the structure observed in our earlier measurement[8] is reproduced in the new scans; the piece of structure in which we have greatest confidence (see Fig. 6) is clearly present in both scans.

V. 3p-LEVEL WIDTHS VERSUS STRUCTURE IN THE M_3 PROFILES

XPS measurements (using Mg $K\alpha_{1,2}$ radiation) for Cu yield[22] a resolved $3p_{1/2}$-$3p_{3/2}$ doublet, each component having a width of ~1.8 eV. As Hüfner and Wertheim[22] noted, this width is large on the scale of structure in the Cu M_3 profile (see Fig. 6), raising the question of whether the structure seen is real. The XPS 3p spectra, of the metals of interest, have been fitted to yield 3p widths and splittings, and the results are tabulated in Table II. The 3p spin-orbit splitting decreases as one goes to the lighter elements and as a result the XPS spectra are not readily resolved into compo-

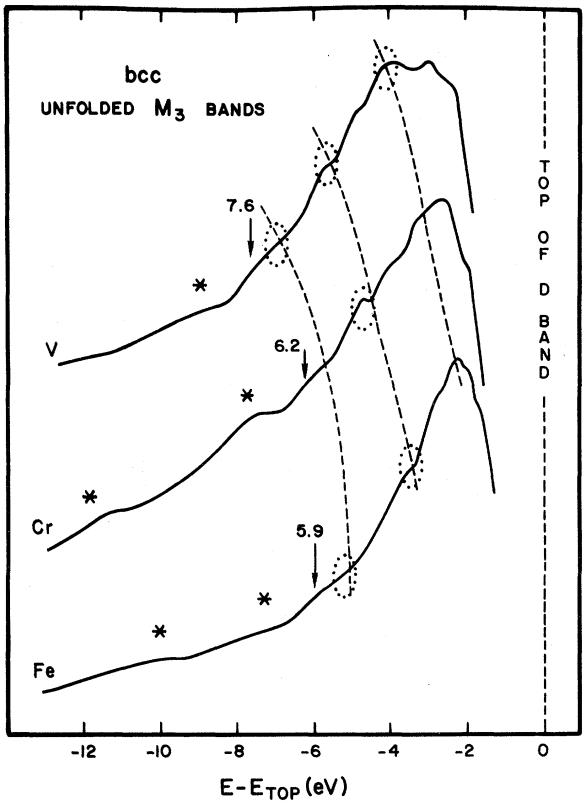

FIG. 7. Comparison of the unfolded M_3 bands of bcc V, Cr, and Fe. The zero of energy is the d-band top as estimated in the text. Dashed lines connecting the profiles indicate the suggested structural correlation. The dotted ovals identify best characterized structure in the raw $M_{2,3}$ spectra. Arrows denote estimated d-band bottom and are labeled with total estimated d-band width. Stars denote expected positions of energy-loss satellites.

TABLE II. Splittings and widths of $3p$ levels.

Metal	Splitting (eV) XPS, experiment	Splitting (eV)[c] Theory	Splitting (eV) Present SXS fits	Splitting (eV)[d] $K\beta_{1,3}$	Full width (eV)[a] XPS, experiment	Corrected[e] width (eV)
Cu	2.4[a]	2.7	2.0	2.0	2.7	1.5
Ni	1.8[b]	2.2	1.9	2.0	···	>1
Co	1.3	1.9	2.3	2.4	2.2	1.0
Fe	1.2	1.6	1.9	1.9	1.8	0.6
Cr	0.8	1.1	1.1	1.3	1.6	0.4
V	0.8	0.7	0.8	1.2	1.6	0.4

[a]J. R. Cuthill and N. E. Erickson (private communication).
[b]J. Hudis (private communication).
[c]Reference 23.
[d]Estimated from unfolding the $K\beta_{1,3}$ x-ray line data of Ref. 31.
[e]Full width less a correction for instrumental broadening.

nents for the metals lighter than Ni. Doublet structures were nevertheless assumed in the fits. With the exception of Co, the deduced splittings and linewidths vary quite smoothly across the row. The splittings are in good quantitative agreement with the $3p$ spin-orbit splittings calculated for the free atoms by Herman and Skillman.[23] This is somewhat surprising for Fe, which suffers the strongest $3d$-$3p$ exchange effects; the out-of-line results seen for Co may be due to these exchange effects. An effort to make multicomponent fits of the Fe and Co spectra appears unproductive at this time largely because, without a detailed theoretical prediction of the "multiplet" spectrum, the fits would be far from unique. The Fe, Co, and Ni M_3 structure, in which we have highest confidence (Figs. 6 and 7), lie further below the main peaks of the spectra than the M_2-M_3 spread indicated by Table II. This suggests that going from a doublet to a more rigorous multicomponent fit will not affect conclusions concerning their presence.

The doublet splittings employed in resolving the M_3 component are listed in Table II. They are not exactly equal to the XPS fitted values. Use of the latter, instead, does not visibly affect the M_3 curves of Figs. 6 and 7. Except for V, the splittings assumed in the present fits agree best with splittings inferred from $K\beta_{1,3}$ spectra ($1s \rightarrow 3p$ transition) which are listed in Table II.

The $3p$-component widths obtained by XPS for Cu and Ni make any structure in their M_3 profiles surprising; smearing theoretical densities of states (DOS) with Lorentzians of these widths pretty well wipes out all the structure. Either, the density of states combined with transition probabilities has sharper structure than the theoretical DOS curves, or the origin of the SXS level widths is not exactly the same as that for the XPS widths. Both factors may be operative: We have no plausible explanation for the apparent substantial deviation from the XPS level widths in the present experiments.

VI. TRENDS IN THE M_3 PROFILES

The M_3 profiles for fcc Fe and Co, as well as those obtained earlier for Ni and Cu, are displayed in Fig. 6; the profiles for bcc V, Cr, and Fe are shown in Fig. 7. The data shown in these figures for bcc Fe and fcc Co were obtained below the Curie temperature; for Ni and fcc Fe, above. The zero of energy of the figures was chosen to be the top of the d bands, not E_F. Appearance potential measurements of Park and Houston[24] were used to estimate the unoccupied d-band widths. The M_3 profiles have broad low-energy tails arising in part from many-body and in part from one-electron effects. As a result, the placement of the bottom of the d bands cannot be done uniquely. Our choice, indicated by the arrows in the figures, is based first on observation of structural correlations between the M_3 profiles and theoretical densities of states and then on structural correlations between the M_3 profiles for metals of like crystal structure. The absolute values of the resulting bandwidths have some uncertainty but the width for one metal, relative to that of another, is well determined.

Correlations between the dominant structure of one M_3 profile, and that for another metal of like symmetry, are suggested by the dashed lines of Figs. 6 and 7. It is foolhardy to take such comparisons too seriously but the correlations between Cu and Ni, among the fcc metals, and between V and Cr, among the bcc, are particularly striking.

VII. BANDWIDTH

One clear feature of Fig. 6 is the minimum in bandwidth at Ni among the fcc metals. This is *independent* of our particular choice of d-band bottoms. This has also been observed by XPS[16] and UPS[17] measurements and is at variance with theory. In Fig. 8, we compare the experimental bandwidths with band-theory predictions, where the X_3-X_5 and H_{12}-H_{25} energy-level differences have been taken

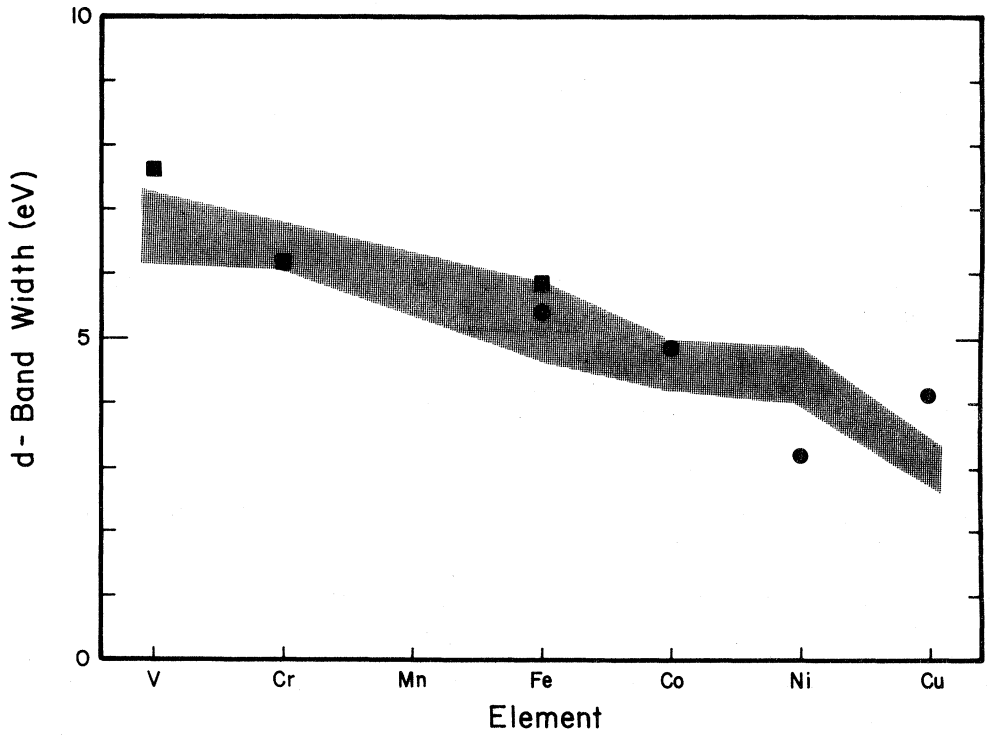

FIG. 8. Comparison of measured and calculated total d-band widths. Squares are for bcc, circles are for fcc experimental results. The shaded area shows the range of theoretical estimates. Sources for the latter are L. Hodges, R. E. Watson, and H. Ehrenreich, Phys. Rev. B 5, 3953 (1972), and to be published, entire series; G. A. Burdick, Phys. Rev. 129, 138 (1963), J. H. Wood, Phys. Rev. 126, 157 (1962), Fe; L. F. Mattheis, Phys. Rev. 134, A192 (1964), V, Cr, Fe, Co, Ni, Cu; Ref. 3, V; M. Yasui, E. Hayashi, and M. Shinizu, J. Phys. Soc. Jpn. 29, 1446 (1970), V, Cr; Ref. 5, Cr; S. Wako and J. Yamashita, J. Phys. Soc. Jpn. 21, 1712 (1966), Fe; Ref. 6, Ni; S. Wakoh, J. Phys. Soc. Jpn. 20, 1894 (1965), Ni.

as the fcc and bcc widths, respectively. Numerically, there are no gross discrepancies between theory and experiment. The spread in theoretical values arises from the use of different classes of crystal potential. Little spread implies fewer band calculations rather than intrinsic agreement between different classes of potentials. Scanning across the row of metals, there is some question of whether theory and experiment agree on the relative bandwidths of V and Cr and whether experiment indicates the Cu width to be greater than theory, but the most serious question is Ni. Inspection of Fig. 7 suggests that the V bandwidth is substantially larger than that of Cr, in contrast with theory. There is some difficulty in placing the Cr spectrum, relative to the others on Fig. 7, because unlike Fe and V, it has a low density of states at E_F. The error associated with this is not greater than $\frac{1}{2}$ eV and an increase of this magnitude in the experimental bandwidth for Cr still leaves Cr-V looking somewhat anomalous.

Granted that theory and experiment are at least in crude agreement for the other metals, theory for Ni predicts too great a bandwidth. This is one of the major unresolved questions facing transition-metal band theory and it is generally thought to be connected with this metal's magnetism.

VIII. COMPARISON WITH OTHER DEEP BAND PROBES AND THEORY

Considerable amounts of experimental data have been obtained using other deep band probes, most notably ultraviolet (UPS) and x-ray (XPS) photoemission. Though differing in such matters as initial state, mode of excitation, and transition probabilities, each of these techniques yields some image of the distribution, in energy, of final-state valence-band holes. The classic UPS studies of Eastman and co-workers of Au,[25] as a function of photon energy, show the UPS spectra approaching the XPS spectrum in character at photon energies of ~50 eV; at much smaller photon energies such matters as k conservation and structure in the density of final photoelectron states above E_F affect the spectrum. We therefore make comparison with UPS spectra plotted as a function of initial-state energy, noting that *coincident structure* in UPS and SXS profiles is likely to be associated with structure in the occupied bands. For UPS results at photon energies up to 11.6 eV, we shall com-

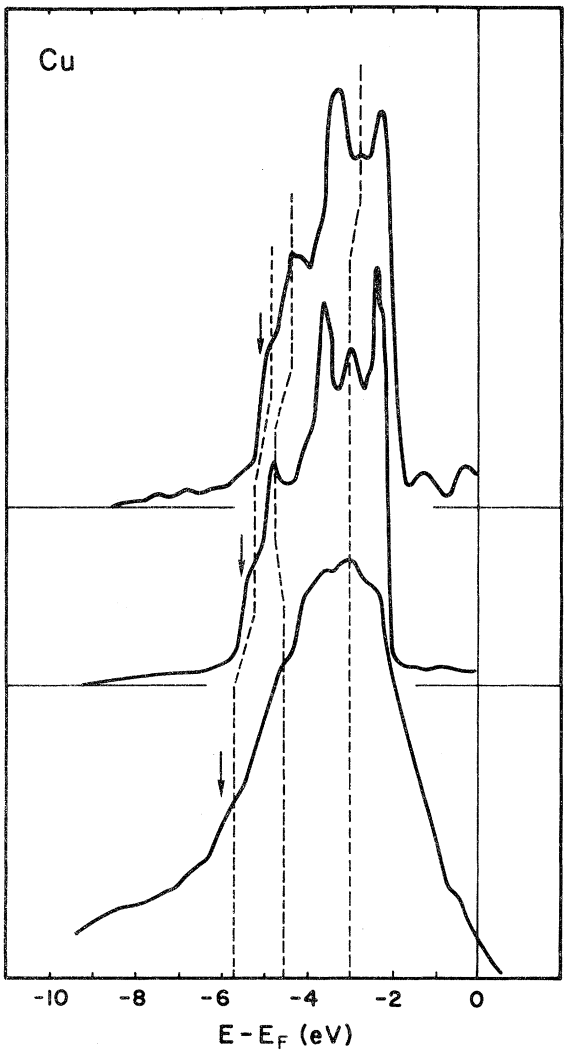

FIG. 9. Comparison of fcc-Cu M_3 profile (lower curve, Ref. 8) with two one-electron estimates of the profile. [Upper curve, Ref. 8; middle curve, D. A. Goodings and R. Harris, J. Phys. C 2, 1808 (1969).] Dashed lines show structural correlations upon which our estimate of the d-band bottom (arrows) is based.

pare with the optical density of states (ODS), which is an effective density of states obtained from a *set* of spectra under the assumption of constant matrix elements and nondirect transitions. This serves as a convenient catalog of structure observed in the low range of photon energies. For higher photon energies, up to 40.8 eV, we use such individual spectra as are available. We have not introduced broadening into the theoretical densities of states. Comparisons for the various metals are displayed in Figs. 9–13. The V and Co comparisons rely on the poorest M_3 and the poorest of photoemission data. The XPS spectrum in Fig. 10 was obtained recently by Szalkowski and Megerle[26] for Fe with a very clean surface. These authors note that their spectrum is in much better agreement with the M_3 spectrum than with earlier XPS results.

Holliday's raw L_3 SXS spectrum for[27] Fe also appears in Fig. 10. The L_3 spectrum involves a $2p$ rather than a $3p$ inner level, and thus is expected to yield much the same information as the M_3 spectrum. $2p$ binding energies are greater,

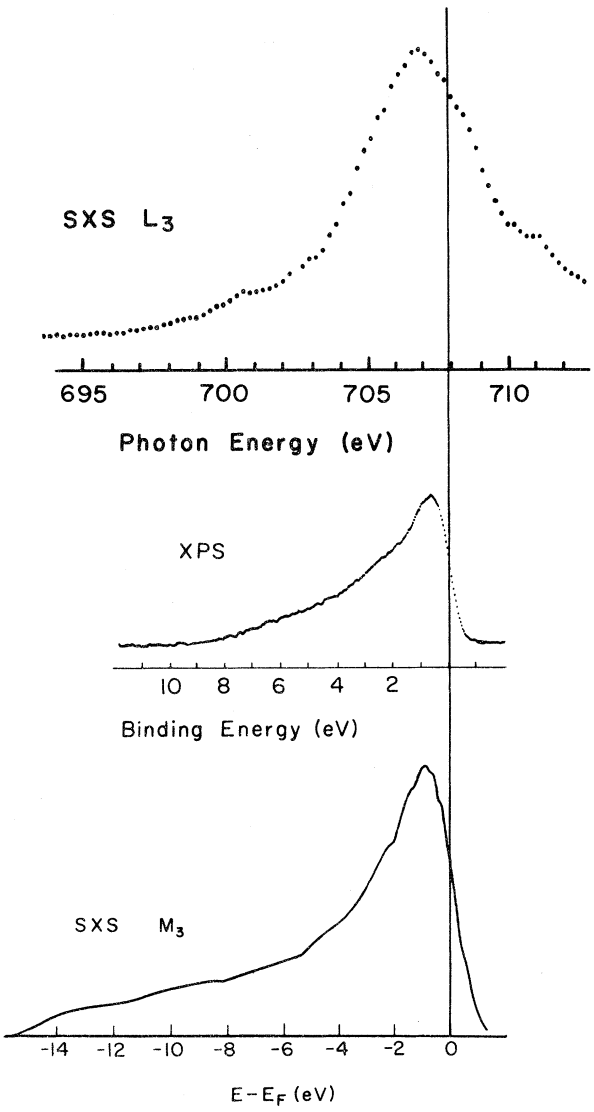

FIG. 10. Comparison of the bcc M_3 profile of Fe at 560°C with the XPS valence-band spectrum (Ref. 26) and SXS L_3 spectrum (Ref. 27). The vertical line indicates the position of the Fermi level. For the XPS spectrum the author's Fermi-level placement has been used. For the SXS L_3 spectrum, the Fermi level has been placed using L_3 adsorption edge and emission band data of S. Hanzely and R. J. Liefeld, in Ref. 13; the latter authors' studies of the L_3 emission profile as a function of excitation energy indicates that the structures in the L_3 spectrum above the Fermi level at 708 and 711 eV are satellites.

from 0.5 to 1.0 keV for the 3*d* metals, as are the spin-orbit splittings. As a result, it is possible to obtain spectra with near-threshold excitation, eliminating much satellite and self-absorption structure. The spectrum displayed was not obtained at threshold, and the Fermi level cannot be placed by eye (see the figure caption for how this was done). There is some question of whether the 2*p* hole widths, relevant to these spectra, are greater or smaller than the 3*p* (XPS results suggest somewhat smaller); however, the limited resolution (~1.0 eV) of the spectrometers available in the energy range of the *L* spectra serves to reduce the resolution of the L_3 spectra. Structure is largely washed out in the L_3 spectrum but in such features as the bandwidth there is good agreement.

It is remarkable the extent to which probes

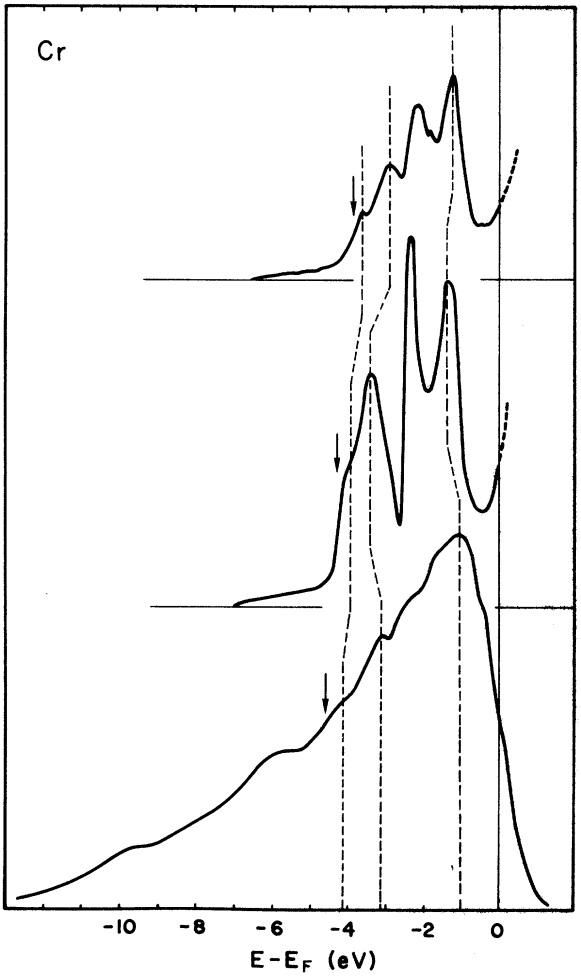

FIG. 11. Comparison of bcc-Cr M_3 profile (lower curve) with two one electron estimates of the total density of states. Middle curve, J. W. D. Connolly, in Ref. 13; upper curve, Ref. 5. Dashed lines show structural correlations upon which our estimate of the location of the *d*-band bottom (arrows) is based.

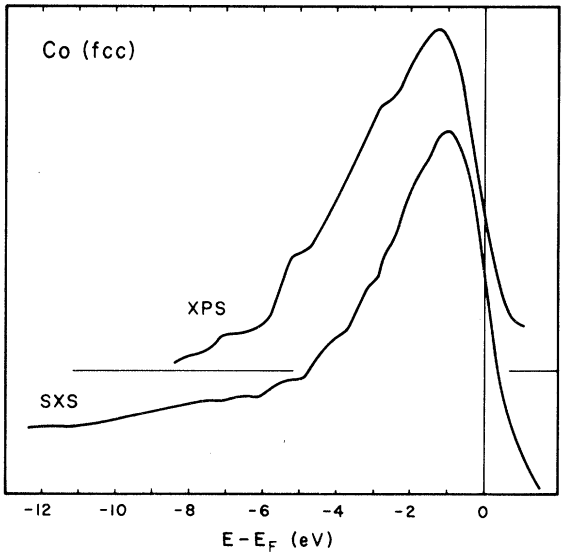

FIG. 12. Comparison of the SXS M_3 and XPS spectra of fcc Co [C. S. Fadley and D. A. Shirley, Phys. Rev. Lett. 21, 980 (1968); and in Ref. 13].

which involve different initial and final states and which sample the metals to different depths yield qualitatively identical results.

APPENDIX: ASSESSMENT OF SAMPLE SURFACE CONTAMINATION

A. Fe

The Fe data at 560 °C were taken after initial measurements at 840 °C (reported elsewhere[10]) which consumed approximately 40 working hours.

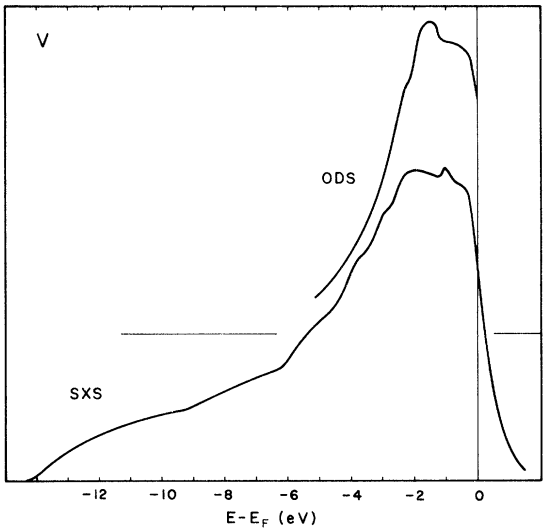

FIG. 13. Comparison of the M_3 spectrum of V with the UPS ODS [D. E. Eastman, Solid State Commun. 7, 1697 (1967)].

Recovery curves for ^{28}Fe indicate that coldwork distortion was completely relieved in this time. The effects of carbon contamination appear to be minimal for the Fe measurements. Weak carbon K-emission bands were detected, in first, second, and third orders only, at photon energies of 276, 138, and 92 eV. The Fe spectra, centered at 51 eV, were therefore unaffected by order overlap. Moreover, comparison of these carbon contaminant bands with measurements by Holliday[29] of carbon K-emission spectra from graphite, inert carbon deposits on Fe, inert carbon inclusions in Fe, and from carbon chemically bound to Fe (the latter showing marked chemical shifts from the former), indicates that the overwhelming bulk, if not in fact all, of the carbon contaminant in the present Fe measurements resided in a thin, chemically inert surface layer. The possibility that the measured Fe $M_{2,3}$ bands were biased by the presence of Fe oxides on the sample surface was checked by scanning the Fe continuum in the spectral region of the third order of the oxygen K band immediately after the measurements at 560 °C. The oxygen K band was undetectable at a background signal-to-noise ratio of 2%. A further check was made by comparing the intensities of the Fe $M_{2,3}$ and third order of the oxygen K bands from a heavily oxidized Fe sample (Fe_3O_4 on Fe) at 560 °C. From the observed oxygen-to-Fe intensity ratio from the oxide, and by assigning the noise level from the Fe-sample oxygen scans as the maximum possible oxygen emission intensity from the Fe sample, we are able to exclude the possibility that radiation from Fe bound to oxygen contributes in detectable amounts to the observed 560 °C Fe $M_{2,3}$-emission spectrum. We further note that the initially heavy oxide layer on the oxidized Fe sample was almost completely eroded away in the region under the electron beam during the course of the oxide measurements. Oxygen scans were not carried out for the Fe measurements at 960 °C.

B. Cr, Co, and V

Weak carbon K bands were observed through third order in the course of the Cr, Co, and V studies as well. They were identical in structure to those observed on Fe, and we believe them to arise from slight, chemically inert deposits on the sample surfaces. Outgassing times were similar in these cases to that of the Fe sample; coldwork damage should not be a factor in these measurements. Oxygen scans were made on the Cr sample, and a weak oxygen K peak was observed. We made no studies of Cr oxides. However, if, as seems reasonable from the photographic survey studies of Skinner, Bullen, and Johnston[30] of the $M_{2,3}$ spectra of the 3d metals and their oxides, the Cr-$M_{2,3}$-to-oxygen-K-band intensity ratio from Cr oxide does not differ materially from that observed by us from Fe_3O_4, then one expects the maximum possible intensity of the Cr-oxide contribution to the observed Cr emission band not to exceed 2% of the total maximum observed intensity. Only if some very sharp and strong feature occurs in the Cr-oxide band (a possibility which the data of Skinner *et al.*[30] appears to rule out) would this contribute to the fine structure observed here in the Cr $M_{2,3}$-emission spectrum. We therefore believe the fine structure observed in the Cr band to be characteristic of Cr metal. The overall shape of the band may be distorted to some slight degree by radiation from Cr atoms chemically bound to oxygen.

No oxygen scans were made on the Co and V samples. We cannot rule out the possibility of oxide distortion of these bands. We note, however, that when the samples were removed from the instrument, each showed bright metallic lustre. Therefore there was no gross oxide buildup, and we feel that in all likelihood the data are characteristic of the bulk metals, and at the least, our bandwidth estimates should be valid.

---

†Present address: Institute for Applied Technology, National Bureau of Standards, Gaithersburg, Md. 20760.

‡Also a consultant with the National Bureau of Standards.

*Work supported by the U. S. Energy Research and Development Administration.

[1]A. V. Gold, L. Hodges, P. T. Panousis, and D. R. Stone, Int. J. Magn. 2, 357 (1971), Fe.

[2]R. A. Tawil and J. Callaway, Phys. Rev. B 7, 4242 (1973), Fe.

[3]D. A. Papaconstantopoulos, J. R. Anderson, and J. W. McCaffrey, Phys. Rev. B 5, 1214 (1972), V.

[4]J. F. Couturier, C. R. Acad. Sci. (Paris) 272, 275 (1971), Cr.

[5]S. Asano and J. Yamashita, J. Phys. Soc. Jap. 23, 714 (1967), Cr.

[6]J. W. D. Connolly, Phys. Rev. 159, 415 (1967), Ni.

[7]A. J. McAlister, R. C. Dobbyn, J. R. Cuthill, and M. L. Williams, J. Phys. Chem. Ref. Data 2, 411 (1973).

[8]R. C. Dobbyn, M. L. Williams, J. R. Cuthill, and A. J. McAlister, Phys. Rev. B 2, 1563 (1970).

[9]A. J. McAlister, M. L. Williams, J. R. Cuthill, and R. C. Dobbyn, Solid State Commun. 9, 1775 (1971).

[10]A. J. McAlister, J. R. Cuthill, R. C. Dobbyn, M. L. Williams, and R. E. Watson, Phys. Rev. Lett. 29, 179 (1973).

[11]N. V. Smith and M. M. Traum, in *Electron Spectroscopy*, edited by D. A. Shirley (American Elsevier, New York, 1972).

[12]N. V. Smith, Phys. Rev. B 3, 1867 (1971).

[13]J. F. Janak, D. E. Eastman, and A. R. Williams, *Electronic Density of States*, edited by L. H. Bennett, Natl. Bur. Stand. (U. S.) Spec. Pub. 323 (U. S. GPO,

Washington, D. C., 1971).

[14]A brief report of these Fe results has already appeared in Ref. 10, where the temperature dependence of the bcc-Fe M_3 profile across the Curie temperature was studied.

[15]J. R. Cuthill, A. J. McAlister, M. L. Williams, and R. E. Watson, Phys. Rev. 164, 1006 (1967).

[16]S. Hüfner, G. K. Wertheim, N. V. Smith, and M. M. Traum, Solid State Commun. 11, 323 (1972).

[17]D. E. Eastman, in Ref. 11.

[18]J. R. Cuthill, Rev. Sci. Instrum. 41, 422 (1970).

[19]Smoothed curves were obtained in the following way: First, background estimates were made for each metal by scanning the continua of neighboring elements having no characteristic structure in the region of the appropriate $M_{2,3}$ spectral complex, and from this data, establishing a "universal" background curve. This background curve was then fitted to the high- and low-energy tails of the raw spectrum and subtracted. A smooth curve was then drawn through the difference in a manner consistent with the standard counting error.

[20]J. L. Robins and J. B. Swann, Proc. Phys. Soc. Lond. 76, 857 (1960).

[21]Spectator hole ($3p$ or valence band) satellites should have been largely removed in the unfolding process. (See Ref. 8.) Some residual satellite structure occurs just above the d bands in the M_3 spectra, and in the L_3 spectra as well. (See S. Hanzely and R. J. Liefeld, in Ref. 13. Both here and in Ref. 8, this structure has been rationalized as due to bound-ejected electron states.) Self-absorption effects should be minimal for the experimental setup used here. [See Refs. 8, 15, and J. R. Cuthill, R. C. Dobbyn, A. J. McAlister, and M. L. Williams, Phys. Rev. 174, 515 (1968).] An additional piece of evidence on the reduction of self-absorption comes from our unpublished study of the $L_{2,3}$ emission edge of Al. By varying the excitation geometry at constant 2.5-keV electron-beam voltage, we can vary the apparent L_2/L_3 edge intensity at will from 0.05 to 0.35. We are, of course, operating in the present measurements at settings favoring low self-absorption. Only a few of the M_3 separation parameters are listed here, in Table II. Complete details will be supplied on request.

[22]S. Hüfner and G. K. Wertheim, Phys. Lett. A 44, 47 (1973).

[23]F. Herman and S. Skillman, *Atomic Structure Calculations* (Prentice-Hall, Englewood Cliffs, N. J., 1963).

[24]With the exception of Cu, which was placed so that its upper d-band shoulder matched that of Ni in energy, the location of the d-band top relative to the Fermi level was taken to be the width of the unoccupied d states as estimated by R. L. Park and J. E. Houston [Phys. Rev. B 6, 1073 (1972)] from their L-shell soft-x-ray appearance potential (APS) measurements. These widths, corrected for instrumental resolution and core-level lifetime width, are 2.0, 1.6, 1.2, 0.6, and 0.3 eV for V, Cr, Fe, Co, and Ni, respectively. This method of placement has been used because it provides probably the best, but more importantly, a consistent experimental estimate. There are obvious interpretational difficulties involved, and it should be noted that for one of the metals considered here, the APS measurements were made under different physical conditions. Specifically, APS measurements were made on ferromagnetic hcp CO. We assume errors arising from this difference, and from differences in sample temperature when the phases are otherwise the same, to be small. The x-ray continuum isochromats for V, Fe, Co, and Ni, as measured by R. R. Turtle and R. J. Liefeld, Phys. Rev. B 7, 3411 (1973), yield unfilled d-bandwidths in reasonable agreement with the APS results; more significantly, the trend with electron-per-atom ratio is the same.

[25]D. E. Eastman and J. K. Cashion, Phys. Rev. Lett. 24, 310 (1970). Comparison between XPS and high-energy UPS data has been made by S. B. M. Hagstrom, in Ref. 11; see also D. E. Eastman, in Ref. 11.

[26]F. J. Szalkowski and C. A. Megerle, Phys. Lett. A 48, 117 (1974).

[27]J. E. Holliday, Adv. X-Ray Anal. 14, 243 (1971).

[28]See, for instance, *Metals Handbook*, edited by T. Lyman (American Society for Metals, Cleveland, 1948), p. 261.

[29]J. E. Holliday, Norelco Reporter 14, 84 (1967).

[30]H. W. B. Skinner, T. G. Bullen, and J. E. Johnston, Philos. Mag. 45, 1070 (1954).

[31]G. A. Bearden and C. H. Shaw, Phys. Rev. 48, 8 (1935).